

## MINORITY CARRIER PROPERTIES OF MICROCRYSTALLINE SILICON THIN FILMS GROWN BY *HW-CVD* AND *VHF-PECVD* TECHNIQUES

S. Okur\*, O. Göktaş, M. Güneş, F. Finger<sup>a</sup>, R. Carius<sup>a</sup>

Department of Physics, Izmir Institute of Technology, Gülbahçe Kampus 35430 Urla-Izmir, Turkey

<sup>a</sup>Institut für Photovoltaik, Forschungszentrum Jülich, GmbH, 52425 Jülich, Germany

Opto-electronic properties of  $\mu\text{-Si:H}$  films prepared by hot-wire/catalytic chemical vapor deposition (HWCVD) and very high frequency plasma enhanced chemical vapor deposition (VHF-PECVD) techniques with various silane concentrations (SC) have been investigated using Raman spectroscopy, the steady-state photocarrier grating technique (SSPG), and the steady-state photoconductivity (SSPC). A correlation between the minority carrier transport properties and the microstructure has been found, using the dependence of the diffusion length ( $L_d$ ) on the SC and Raman intensity ratio ( $I_c^{RS}$ ) representing crystalline volume fractions.  $I_c^{RS}$  changes from 0.22 to 0.77.  $L_d$  increases with increasing  $I_c^{RS}$ . It peaks around 0.5 with a maximum value of 270 nm, then decreases. Similar dependences of  $L_d$  on  $I_c^{RS}$  were obtained for films prepared by both HWCVD and VHF-PECVD. However, the grating quality factor measured on highly crystalline HWCVD films is substantially smaller than that found for VHF-PECVD films, indicating a relatively higher surface roughness present in the highly crystalline HWCVD films.

(Received December 9, 2004; accepted January 26, 2005)

*Keywords:* Raman spectroscopy, Microcrystalline silicon thin film, Diffusion length, Steady state photocarrier grating technique

### 1. Introduction

Both hot-wire/catalytic chemical vapor deposition (HWCVD) [1-2] and plasma enhanced chemical vapor deposition (PECVD) [3,4] techniques have been successfully used, in the past few years, to prepare microcrystalline silicon ( $\mu\text{-Si:H}$ ) films, with a precise control of the crystalline volume fraction. Recent experimental results on  $\mu\text{-Si:H}$  materials produced by these techniques show that the best solar cell performance is obtained in a microcrystalline growth regime close to the transition to amorphous growth conditions [5,6]. The crystalline volume fraction in these types of film is usually inferred from Raman Spectroscopy for structural analysis [7]. The steady-state photocarrier grating technique (SSPG) and the steady state photoconductivity (SSPC) have been used for the characterization of both minority and majority carrier transport properties of a-Si:H and  $\mu\text{-Si:H}$  films, or materials between these two regimes [4-6]. A correlation between the electronic and structural properties in relation to the deposition conditions around the transition region from  $\mu\text{-Si:H}$  to a-Si:H growth is an important issue for improving solar cell efficiency.

In this work, we have investigated the relationship between the diffusion length measured with SSPG and the crystalline volume fractions obtained from Raman Spectroscopy, for  $\mu\text{-Si:H}$  films which were grown using various silane concentrations, The films, prepared by both HWCVD and PECVD techniques, ranged from highly crystalline to nearly amorphous.

---

\* Corresponding author: salihokur@iyte.edu.tr

## 2. Experimental details

Undoped hydrogenated microcrystalline silicon ( $\mu\text{c-Si:H}$ ) films were fabricated using both the PECVD technique with a very high frequency of 95 MHz and a plasma power of 8W, and the HWCVD technique with tantalum filaments operating at temperatures between 1650 and 1800 °C. The substrate temperatures were varied between 185 and 220 °C, and the silane concentrations ( $\text{SC} = [\text{SiH}_4]/[\text{SiH}_4+\text{H}_2]$ ), between 2% and 10%. Experimental details about the film growth are given in [1,4]. A standard SSPG system was used to measure the diffusion length [8,9]. A He-Ne laser with wavelength of 633 nm was used to measure the SSPG small-signal photocurrent for generation rates,  $G$ , between  $10^{18}$  and  $10^{22} \text{ cm}^{-3} \text{ s}^{-1}$ . The applied dc voltage (10V) was in the Ohmic region, for coplanar contacts with a gap of 0.5 mm deposited on the  $\mu\text{c-Si:H}$  samples. The photocurrent ratio ( $\beta$ ), measured as function of the grating period ( $\Lambda$ ), was independent of the applied dc voltage up to 10V. A detailed experimental configuration and procedure for the SSPG technique used here is given in previous reports [8,9].

## 3. Results and discussion

Laser light with a wavelength of 488 nm was used to perform the Raman scattering experiments. The crystalline volume fraction ( $I_C^{\text{RS}}$ ) was calculated from the integrated intensity ratio,  $I_C^{\text{RS}} = (I_{520} + I_{500}) / (I_{520} + I_{500} + I_{480})$ , by de-convolution of the Raman spectral data into three characteristic Raman peaks positioned at 480, 500 and 520  $\text{cm}^{-1}$ .  $I_C^{\text{RS}}$  was used as a semi-quantitative measure of the crystalline volume fraction. Fig. 1a shows the  $I_C^{\text{RS}}$  of films prepared in the transition region from amorphous to microcrystalline growth, using a SC from 2.5% to 10%, for both HWCVD and PECVD films. The  $I_C^{\text{RS}}$  exhibits a similar dependence on the SC for both type of films, and decreases as the SC increases.

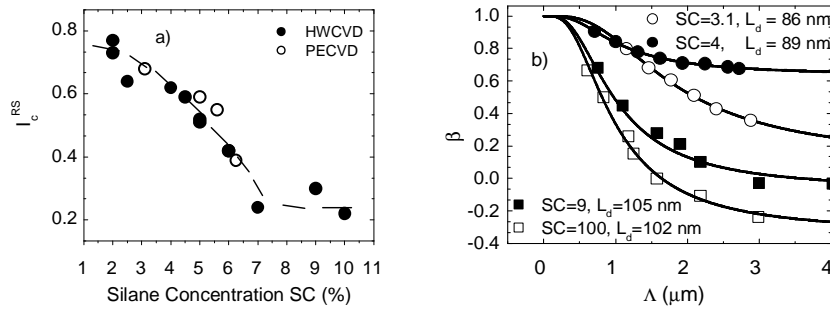


Fig 1: (a)  $I_C^{\text{RS}}$  vs SC (the dashed line is a guide to the eye) and (b)  $\beta$  versus grating period  $\Lambda$  for HWCVD (filled symbols) and PECVD (open symbols) films prepared in the microcrystalline (low SC) and amorphous (high SC) regimes. The lines are nonlinear least square fits to the Equation 1 given in Reference 9.  $L_d$  (diffusion length) and  $\phi$  (grating quality parameter) are the fitting parameters.

A typical  $\beta$  versus  $\Lambda$  is shown in Fig. 1b, for films prepared in the low (amorphous) and highly crystalline regions, for both HWCVD and PECVD samples.  $L_d$  and the grating quality fit parameter  $\phi$  were obtained from a nonlinear least square fit method to Eq. 1 of reference [9]. The  $L_d$  values were around 100 nm and 85 nm for low-crystalline and high-crystalline regions, respectively. However, a major difference was found for the fitting parameter  $\phi$ , which was rather smaller in highly crystalline regions. The  $L_d$  values obtained for other intrinsic  $\mu\text{c-Si:H}$  films are summarized as a function of the crystalline volume fraction present in the material. They are shown in Fig. 2a for films prepared by both types of method. For the pure a-Si:H sample,  $I_C^{\text{RS}}=0$ ,  $L_d$  was around 105 nm. It increased with increasing  $I_C^{\text{RS}}$  and peaked at around 270 nm for an  $I_C^{\text{RS}}$  of 0.5. This region corresponds to the transition from microcrystalline to amorphous growth. For both HWCVD and VHF-PECVD samples, the highest  $L_d$  values were obtained in this transition region. Further increases in  $I_C^{\text{RS}}$  cause a substantial decrease in the  $L_d$  values. In the highly crystalline region, the defect density has been suggested to increase, due to the etching effect of hydrogen at the grain boundary walls

[10]. This causes an increase in the density of recombination centers for both electron and holes. Therefore, the  $L_d$  values for the minority carriers (holes) decrease with increasing  $I_C^{RS}$ . In Fig. 2b, the SSPG grating quality factor ( $\gamma_0$ ) is shown as a function of  $I_C^{RS}$ . The  $\gamma_0$  value was obtained as  $\gamma_0 = (\phi / \gamma_d \gamma)^{1/2}$ , where  $\phi$  is the SSPG fitting parameter obtained from the fit to the experimental  $\beta$  versus  $\Lambda$  curve in Fig. 1b and  $\gamma$  is the exponent of the photoconductivity  $\sigma_{ph}$  power law variation with the generation rate  $G$ , and  $\gamma_d$  is the dark conductivity reduction factor defined as  $\gamma_d = \sigma_{ph} / (\sigma_{ph} + \sigma_{dark})$  [9,11]. In the low-crystalline region, the  $\gamma_0$  values were high for both HWCVD and VHF-PECVD films. They decreased from 0.95 to 0.75 and from 0.9 to 0.5 after the transition to microcrystalline growth region, for HWCVD and VHF-PECVD films respectively. It can be inferred from the results that HW-CVD grown films at the highly crystalline region exhibit a higher surface roughness [12].

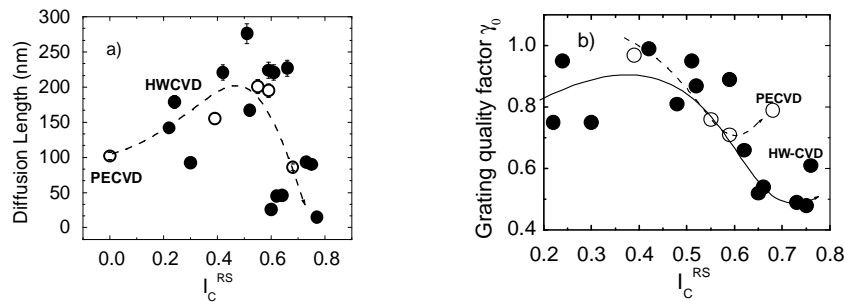


Fig. 2: (a) Diffusion length  $L_d$  versus  $I_C^{RS}$  for HWCVD (filled circles) and PECVD (open circles) films. The lines are guides to the eye, (b) Grating quality factor  $\gamma_0$  as a function of  $I_C^{RS}$  for HWCVD (filled circles) and (open circles) PECVD films. The lines are guides to the eye.

Finally, the minority carrier hole  $\mu_p^0 \tau_p^R$  product, calculated using the  $L_d$  values in Fig. 2a, and the majority carrier electron  $\mu_n^0 \tau_n^R$  product, obtained from the SSPC measurements, are shown in Fig. 3a and Fig. 3b respectively, as a function of the generation rate for both HWCVD and PECVD samples. It is clearly seen that majority carrier  $\mu_n^0 \tau_n^R$  products are higher than minority carrier  $\mu_p^0 \tau_p^R$  products, for both types of intrinsic  $\mu c$ -S:H film, indicating electron dominated transport. However, the HWCVD films show a better minority carrier  $\mu_p^0 \tau_p^R$  product than the VHF-PECVD films. The ratio,  $b = \mu_n^0 \tau_n^R / \mu_p^0 \tau_p^R$ , also called Fermi level parameter, changed between 5 and 8 for HWCVD films and between 26 and 354 for VHF-PECVD films. This indicates that a more n-type character is present in VHF-PECVD films. It is also important to note that the effect of instabilities due to adsorption and oxidation on the dark Fermi level has to be taken into account in comparing both the majority and the minority carrier transport properties. In-diffusion of atmospheric gases, strongly affects the dark conductivity and the ESR measurements, by shifting the dark Fermi level when samples are left in air [13]. Therefore, this comparison has to be done under similar experimental conditions, where the effects of atmospheric gases are not present in intrinsic  $\mu c$ -Si:H films.

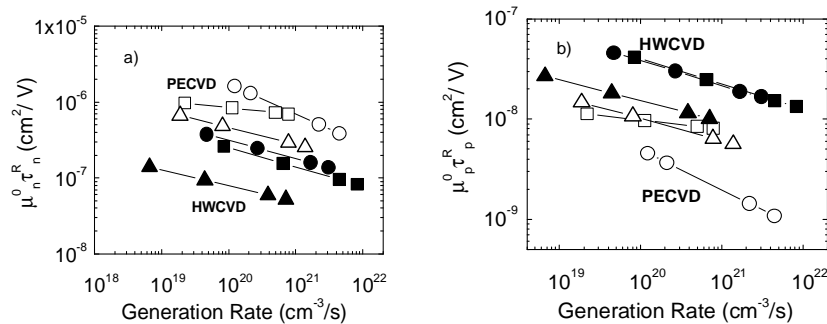


Fig. 3: a) Majority carrier  $\mu_n^0 \tau_n^R$  product and b) minority carrier  $\mu_p^0 \tau_p^R$  product obtained by SSPC and SSPG experiments for HWPECVD films (filled symbols) and PECVD films (open symbols). HWCVD films:  $\bullet$  (SC=4.5,  $I_C^{RS}=0.59$ ,  $b=6$ ),  $\blacksquare$  (SC=5,  $I_C^{RS}=0.51$ ,  $b=8$ ) and  $\blacktriangle$  (SC=7,  $I_C^{RS}=0.24$ ,  $b=5$ ), PECVD films:  $\circ$  (SC=3.1,  $I_C^{RS}=0.68$ ,  $b=355$ ),  $\square$  (SC=5,  $I_C^{RS}=0.59$ ,  $b=85$ ),  $\Delta$  (SC=6.25,  $I_C^{RS}=0.39$ ,  $b=6$ ).

## 5. Conclusions

The minority carrier diffusion length of intrinsic  $\mu\text{-Si:H}$  films deposited by both the VHF-PECVD and the HW-CVD method, with different SCs, was measured using the SSPG technique. The crystalline volume fraction obtained from Raman experiments changed from 0.22 to 0.77 for SCs between 10% and 2% respectively. The diffusion length  $L_d$  obtained from SSPG experiment showed a maximum value of 271 nm for  $I_C^{RS}$  around 0.5. It then decreased with increasing  $I_C^{RS}$ , probably as a result of the increasing defect density detected by both PDS and DBP sub-bandgap absorption [14] and ESR [10] experiments. The grating quality factor  $\gamma_0$  decreased substantially from 0.90 to 0.50 for HWCVD films, and from 0.95 to 0.75 for PECVD films, after the transition to the microcrystalline regime, indicating a relatively higher surface roughness in HWCVD films. The Fermi level parameter  $b$  obtained as a result of  $\mu_n^o \tau_n^R$  product analysis for both types of intrinsic  $\mu\text{-Si:H}$  film shows that the measured undoped films are slightly n-type.

## Acknowledgements

This joint project is partially supported by the International Bureau of the BMBF, Germany under project number 42.4.I3.2.A and the Scientific and Technical Research Council of Turkey (TÜBİTAK) under project number TBAG-U/14.

## References

- [1] Klein, F. Finger, R. Carius, T. Dylla, B. Rech, M. Grimm, L. Houben, M. Stutzmann, *Thin Solid Films* **430**, 2002 (2003)
- [2] C. Niikura, S.Y. Kim, B. Drevillon, Y. Poissant, P. Rocai Cabarrocas, J.E. Bouree, *Thin Solid Films* **395**, 178 (2001).
- [3] A. Shah, E. Vallat-Sauvain, P. Torres, J. Meier, U. Kroll, C. Hof, C. Droz, M. Goerlitzer, N. Wyrsh, M. Vanacek, *Mater. Sci. Eng. B* **69/70**, 219 (2000).
- [4] O. Vetterl, F. Finger, R. Caius, P. Hapke, L. Houben, O. Kluth, A. Lambertz, A. Mück, B. Rech, H. Wagner, *Solar Energy Materials Solar Cells*, **62**, 97 (2000).
- [5] S. Klein, F. Finger, R. Carius, B. Rech, L. Houben, M. Luysberg, M. Stutzmann, *Mat. Res. Soc. Symp. Proc.*, **715**, A26.2 (2002).
- [6] C. Niikura, Y. Poissant, M. E. Gueunier, J. P. Kleider, J. E. Bourée, *J. Non-Crystalline Solids* **299**, 1179 (2002).
- [7] L. Houben, M. Luysberg, P. Hapke, R. Carius, F. Finger, H. Wagner, *Phil. Mag. A* **77**, 1447 (1998).
- [8] R. Ritter, E. Zelodov, K. Weiser, *J. Appl. Phys.* **62**, 4563 (1987).
- [9] S. Okur, M. Güneş, O. Gökteş, F. Finger, R. Carius, *J. Materials Science: Materials in Electronics* **15**, 187, (2004).
- [10] F. Finger, S. Klein, T. Dylla, A. L. Baia Neto, O. Vetterl, R. Carius, *Mat. Res. Soc. Symp. Proc.*, **715**, A16.3 (2002).
- [11] C. Droz, M. Goerlitzer, N. Wyrsh, A. Shah, *J. Non-Crystalline Solids* **266**, 319 (2000)
- [12] R. Brüggemann, *App. Phys. Lett.*, **73**, 499 (1998).
- [13] F. Finger, R. Carius, T. Dylla, S. Klein, S. Okur, M. Güneş, *IEE Proc.- Circuit Devices S., Special Issue: Amorphous and Microcrystalline Devices* **150**, 300 (2003).
- [14] M. Güneş, O. Gökteş, S. Okur, N. Işık, R. Carius, C. Klomfass, F. Finger, *J. Optoelectron. Adv. Mater.* **7**(1), 161 (2005).